Proceedings of ICMM2005:
3rd International Conference on Microchannels and Minichannels
June 13-15, 2005, Toronto, Ontario, Canada

ICMM2005-75205

SPECTROGRAPHIC MICROFLUIDIC MEMORY

David Erickson[a,c], Baiyang Li[a], James R. Adleman[a], Saurabh Vyawahare[b], Stephen Quake[d], Demetri Psaltis[a]

[a] Department of Electrical Engineering, California Institute of Technology, Pasadena, California, 91125
Email: lby@caltech.edu (B. Li), jadleman@sunoptics.caltech.edu (J. Adleman), psaltis@caltech.edu (D. Psaltis)

[b] Department of Applied Physics, California Institute of Technology, Pasadena, California, 91125
Email: saurabhv@its.caltech.edu (S. Vyawahare)

[c] Department of Mechanical and Aerospace Engineering, Cornell University, Ithaca, New York, 14853
Email: de54@cornell.edu

[d] Department of Bioengineering, Stanford University, Stanford, California, 94305
Email: de54@cornell.edu

ABSTRACT

Recent advancements in micro- and nanoscale fluidic manipulation have enabled the development of a new class of tunable optical structures which are collectively referred to as optofluidic devices. In this paper we will introduce our recent work directed towards the development of a spectrographic optofluidic memory. Data encoding for the memory is based on creating spectrographic codes consisting of multiple species of photoluminescent nanoparticles at discrete intensity levels which are suspended in liquids. The data cocktails are mixed, delivered and stored using a series of soft and hard-lithography microfluidic structures. Semiconductor quantum dots are ideally suited for this application due to their narrow and size tunable emission spectra and consistent excitation wavelength. Both pressure driven and electrokinetic approaches to spectral code writing have been developed and will be experimentally demonstrated here. Novel techniques for data storage and readout are also discussed and demonstrated.

INTRODUCTION

Unlike electronic systems, which can generally be reprogrammed at will, most existing optical systems are limited in their adaptability to the relatively small changes in refractive index achievable through application of electric, acoustic or mechanical strain fields. "Optofluidic" devices on the other hand seek to take advantage of recent advancements in micro- and nano-scale fluidics to deliver liquids directly into the optical structures. This provides an order of magnitude increase in the achievable $\Delta n/n$ enabling flexible fine-tuning and even dynamic reconfiguration of optical circuits in addition to traditional microfluidic capabilities such as distribution of chemicals to be analyzed, and temperature stabilization. Examples of such devices which have recently been developed include adaptable photonic crystal lasers [1], fluid-fluid waveguides [2] switches [3] and electrowetting tuned optical fibers [4]. The capabilities in terms of fluidic control, mixing, property and size tuning (e.g. index of refraction) afforded by microfluidics provides an ideal platform upon which to build such devices.

The recent development of scalable multilayer soft-lithography [5] for highly integrated microfluidic devices has led to renewed interest in fluidic memory devices, through either discrete binary sample storage (*e.g.* containing a colored dye or not) [6] or low Reynolds number fluidic flip-flops which exploit the non-linear behavior of viscoelastic polymer solutions [7]. One drawback of existing devices is that information storage density (on the order of 50 Bs/cm^2) tends to be low compared with exiting optical storage mechanisms, which for 4.6GBytes DVDs is roughly 50 MBs/cm^2. While downscaling the fluidically defined feature sizes is an obvious technique for increasing the memory density it does not provide an obvious route by which such memories could exceed the performance of existing devices purely by downsizing. The unique ability of microfluidics to deliver and mix discrete samples of different components in precise ratios does provide the opportunity to exploit spectral multiplexing optical encoding. Such optical multiplexing techniques have been recently used for massively parallel DNA or protein sequencing [8], and even proposed as an info-ink to replace exiting barcodes [9].

The principal behind spectral encoding involves creating discrete information packets which contain different intensity levels of different photoluminescent nanoparticles. For example 10 different intensity levels of an individual species provides 10 different codes which can then be increased exponentially by increasing the number of individual species. Under such a scheme the equivalent number of bits in a single information packet, N, is described by Eq. (1),

$$N = \log_2(I^M - 1) \qquad (1)$$

where I is the number of intensity levels and M is the number of individual species (though not significant in terms of information density the -1 accounts for the fact that the all zero code cannot be distinguished from the background and therefore would be an ambiguous result). The use of 10 different intensity levels with 10 individual species would provide 10^{10}-1 individual codes equivalent to slightly more than 33-bits in a single information packet. As such shrinking down fluidic storage units to the micron-scale could yield similar or even greater storage density than conventional DVDs.

Semiconductor quantum dots [10] are ideal candidates as photoluminesent particles for such an application. Traditional organic dyes tend to exhibit relatively broad FWHM emission spectra and require optical pumping at different wavelengths (*i.e.* different dyes are excited at different wavelengths). Quantum dots on the other hand exhibit very narrow emission spectra, the peak wavelength of which is tuned by changing the particle size (*i.e.* by adjusting the quantum confinement conditions, for details see [10]). An additional feature of quantum dots, essential for this application, is that they can all be excited from the within the UV-Blue range allowing for a single illumination source to be used which can be easily filtered out during data reading.

Here we will introduce our initial work directed towards the development of high density optical memories based on mixtures of quantum dots suspended in liquids and mixed, delivered and stored using microfluidic structures. Some of the key technologies required for the development of a fully functional quantum dot microfluidic memory are demonstrated. Both pressure driven and electrokinetic approaches to spectral coding have been experimentally developed and will be discussed. Techniques for data storage and subsequent optical readout including be discussed including a unique nanowell electrostatic confinement scheme.

EXPERIMENTAL SETUP AND CHIP FABRICATION

All microfluidic transport visualization was conducted on a florescence microscopy setup comprising of an inverted microscope, 100W mercury broadband illumination source, and a specially designed quantum dot filter (Chroma Technology Corp., Rockingham, VT; excitation: bandpass 400nm/120nm emission: longpass 500nm) which allowed for broad illumination of the sample from the UV to the blue and good transmission for green and longer wavelengths. Images were captured on a color CCD camera and spectral measurements were taken using an optical fiber spectrometer (Ocean Optics, Inc.).

Pressure driven transport was controlled using a series of on-chip valves integrated onto the chip, using the multilayer soft lithography technique mentioned earlier [5]. Briefly the chip consists of a thick control and thin membrane like flow layer both of which are fabricated in PDMS using standard rapid prototyping/soft lithography protocols (for details see the Duffy et al. [11]). Chip assembly consists of bonding the upper control layer to the lower flow layer, punching fluidic access holes and then bonding the assembly to a coverslip thereby enclosing the lower flow layer. External solenoid valves control the air pressure delivered to the control channels which, when actuated, locally collapse the flow channel acting as an effective gate valve.

PRESSURE DRIVEN SPECTRAL CODE WRITTER

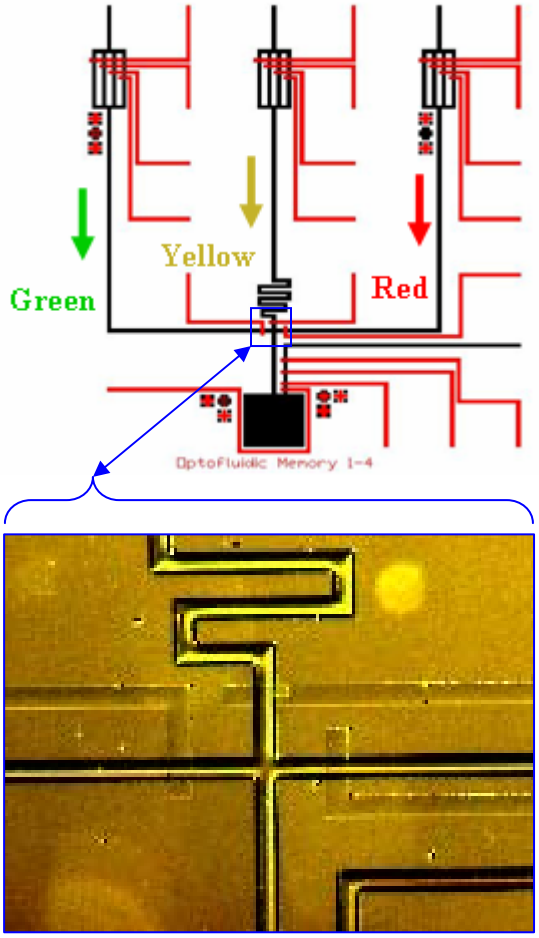

Figure 1: Schematic of pressure driven spectral code writer designed for use with 3 different quantum dot species (Green 525nm, Yellow 565nm and Red 605nm). The red lines are representative the control layer while the black lines show the flow layer. Spectral codes of different species and ratios are generated by opening or closing the appropriate control valves on the parallel channel resistive flow elements. Detail shows closeup view of both the flow and control layers at the intersection.

The electrokinetic chips were also constructed using standard rapid prototyping/soft lithography protocols however comprised of only a single flow layer. Voltages on the order of 1000V were generated using a high voltage power supply (Kepco Power Supply) and switching and voltage adjustment was done through a series of external, custom built electronics.

Applied voltages were coupled to the fluidic system via an electrical harness containing a series of platinum wires which were manually placed in the fluid reservoirs.

Figure 1 shows a schematic outline of the initial pressure driven chip designed for writing discrete intensity levels of three different species of commercially available quantum dots (QDot Corp.: 525nm Green, 565nm Yellow and 605 nm Red). The red lines in the figure are representative of the channels on the control layer and the black lines represent those on the flow layer. A single storage cell is located at the bottom. Each individual delivery channel contains a writing control element consisting of a series of parallel channels (not shown to scale in the diagram) in series with the main channel. The control element serves as an effective stepwise variable flow resistor in that opening each channel reduces the flow resistance and therefore increases the volume flow rate in a stepwise manner. Since the intensity of the individual species is proportional to the volume flow rate into the storage unit the resistance element allows for the writing of discrete intensity levels.

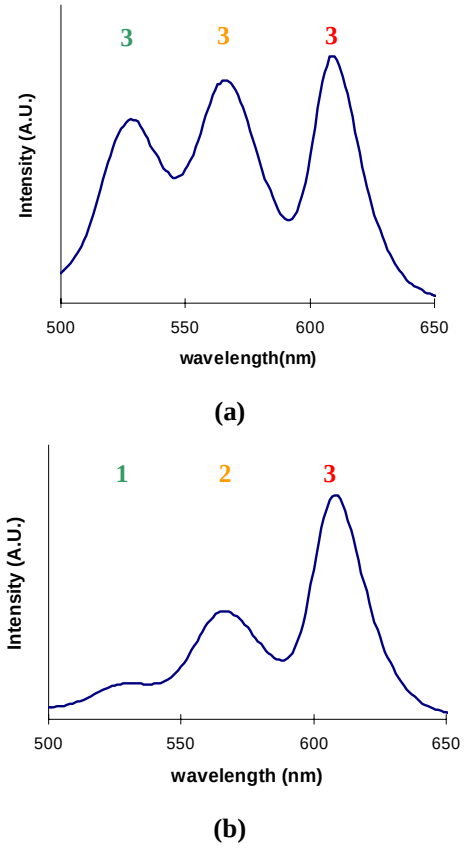

Figure 2: Measured spectrum for 3 species, 4 intensity level optical code approximately corresponding to (a) {G3, Y3, R3} and (b) {G1, Y2, R3}.

Sample spectral codes written with the device and recorded in the storage cell are shown in Figure 2. Two examples are demonstrated corresponding to approximate codes of (a) Green 3, Yellow 3 and Red 3 and (b) Green 1, Yellow 2, and Red 3. In general it was found that while the resistance control elements were successful at writing discrete codes, balancing the channels such that the same number of open elements constituted the same flow rate in each channel (*i.e.* such that each channel had identical inherent resistance) proved difficult. More precise techniques for pressure driven code delivery, including peristaltic pumping, are currently being explored. As can also be seen in Figure 2 heterogeneity in the quantum dot size distribution (resulting in a larger FWHM for individual species) is more pronounced for some colors than others leading to differences in the observed intensity maximum.

ELECTROKINETIC BASED CODE WRITTING

On the 10s of microns scale relatively high flow rates and excellent control can be obtained in microfluidic systems using the pressure driven technique described above. As the channel scale is downsized however such systems have a well known limitation in that the pressure required to maintain a constant flow velocity is inversely proportional to the channel height squared (for a low aspect ratio channel, for square channels the effect is more dramatic). As channels on the order of 100 nanometers or smaller will likely be required to increase memory density to that of existing data storage techniques pressure driven flow may bottleneck the writing speed of the system. Electrokinetic systems however rely on a body force applied at the liquid solid surface, as opposed to across the fluidic cross section, and therefore in general the flow velocity does not scale with channel size (until such time as double layer overlap occurs) and has therefore an inherent advantage for nanoscale fluidics. Additionally since switching is controlled electrically, as opposed to mechanically, setting up and writing of codes can potentially be much quicker, in principal limited only by the viscous response of the fluid.

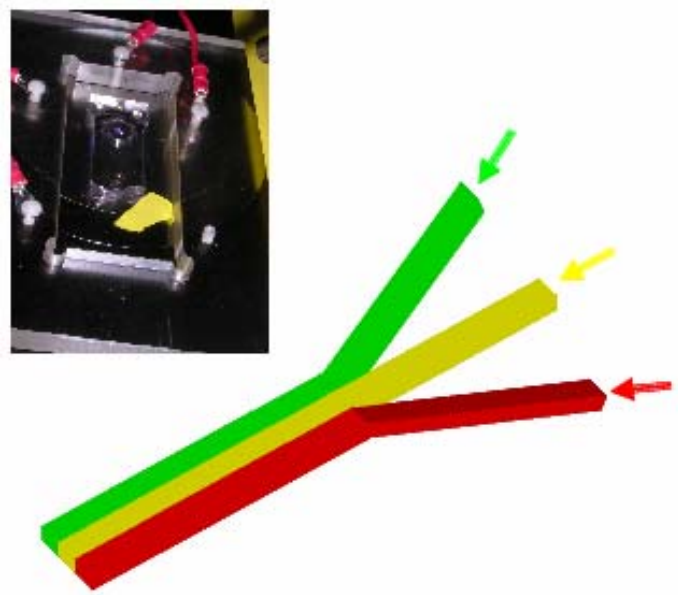

Figure 4: (Left) Chip layout showing electrical harness. (right) Electrokinetic laminar flow streams. The mixing ratio of the memory packets are controlled by adjusting the voltages at the dot reservoirs.

Figure 4 below shows a 3D schematic of the continuous flow electrokinetic technique with an inset showing the chip in the electrical harness (electrical infrastructure not shown). Voltages used here were on the order of 1000V due to the

relatively large size of the chip (several centimeters). In the electrokinetic technique codes are written by adjusting the voltage at the inlet reservoir to predefined levels (*i.e.* lowering the voltage applied to the green reservoir relative to the red reduced its flow rate and thus its intensity level in the information packet). All of the spectra were measured at a distance downstream of the channel to ensure homogeneous mixing.

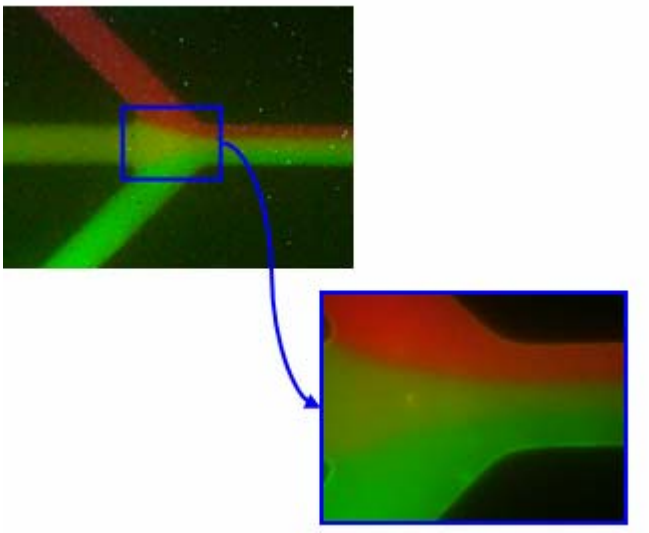

Figure 5: On-line electrokinetic writing of 3 species spectral codes with 1000V applied at each inlet and the outlet grounded. Channel widths are 50 microns and the total length of the system was 3cm.

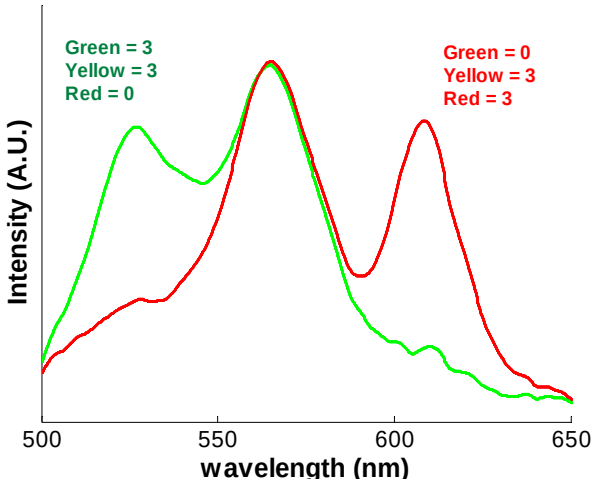

Figure 6: Sample spectra for two different codes taken using the electrokinetic writing technique.

Figure 5 shows continuous flow on-line experiments with each of the 3 parallel mixing stream colors clearly visible. In these cases 1000V is applied at each inlet so equal ratios of all quantum dot species are obtained. The inset shows a close-up view at the intersection prior to downstream diffusive homogenization and spectral readout. Figure 6 shows two overlapping spectral codes written with the technique and measured downstream of the intersection. As can be seen good repeatability in intensity levels can be obtained from code to code.

NANOWELL TRAPPING SCHEME

As alluded to earlier, the other major technology required to create a practical fluidic memory device is a non-volatile, re-writeable, storage mechanism which can be manufactured at densities comparable with existing optical memories. While creative valve designs have proven successful in low density situations, the ratio of valve area to storage area tends to be low and it requires downsizing the size of the transport system to that of the storage area (*i.e.* to scale down the size of the storage chambers requires scaling down all the transport fluidics to the same scale). As such we are developing a nanowell trapping scheme, similar to that shown in Figure 7 in which quantum dot memory packets are electrostatically trapped in small nanowells where they can stored, read and then easily removed when the memory is to be erased. In this case we use streptavidin conjugated colloidal quantum dots which we have observed to support a negative charge at pH ~ 8.3.

In principal the nanowell trapping scheme works by creating a series of electron-beam lithography defined storage wells in an insulating layer of PMMA. Each nanowell is made individually electrically addressable via an optically transparent chemical etch defined Indium Tin Oxide (ITO) layer on a glass substrate. PDMS fluidics are then used to deliver the quantum dot packets to the general area of the targeted storage site and the applied field is used attracted to the quantum dots to the appropriate storage well. The quantum dots can then be rejected into the bulk (erase step) by reversing the polarity. The membrane layer serves as an antidiffusive barrier through which the quantum dots cannot diffuse through unless directed by the applied electric field (as has been demonstrated by Dai *et al.* [12]). The major limitation of such a scheme is that as the applied potential between the ITO electrode and the ground must be less than 1V to remain below the activation energy for electrolytic bubble generation. Additionally the use of an electric field based trapping technique prohibits the use of an electrokinetic transport technique, however since the size of the storage wells and fluidic delivery circuits can be decoupled nanoscale transport may not be required. An additional difficulty expected with electrostatic trapping of quantum dot cocktails is the observed difference in electrophoretic mobility with nanoparticle size (and therefore color). To alleviate this a charge equalization scheme has been proposed in which oligonucleotides of varying length are conjugated to the streptavidin coated quantum dots to equalize the charge/drag ratio.

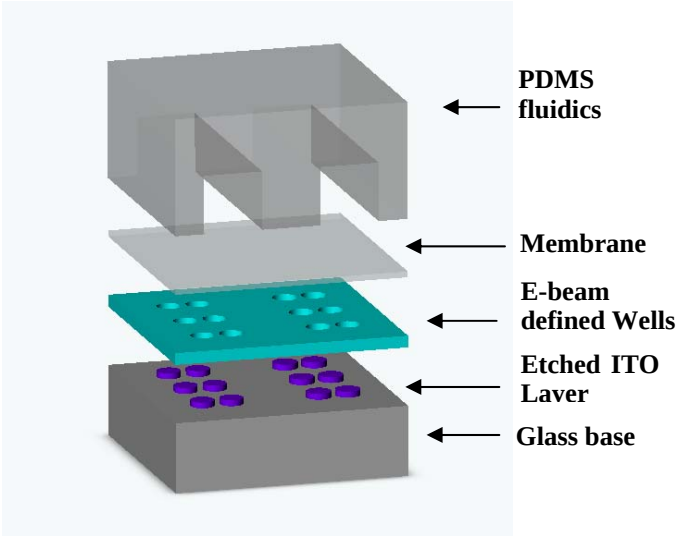

(a)

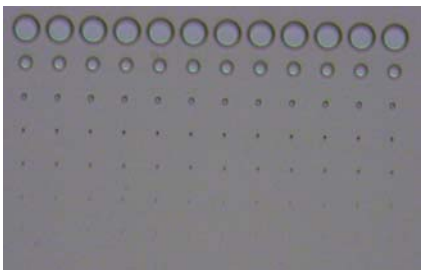

(b)

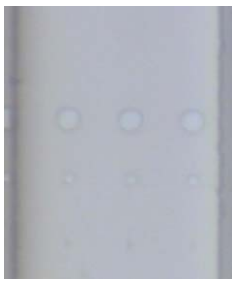

(c)

Figure 7: (a) Conceptual 3D Overview of Nanowell Trapping Scheme. Bottom layer consists of Indium Tin Oxide (ITO) doped glass etched so as to create individually addressable nanoscale storage pads (ITO patterned wires not shown). A transparent insulating layer of PMMA serves to define the storage wells and to concentrate the trapping electric field and the membrane layer serves as a anti-diffusive barrier. PDMS fluidics deliver the dots to general region of the trapping desired storage cell. (b) Electron beam lithography defined hole trapping hole array in PMMA on ITO doped glass. Sizes range from 10μm to 500nm (c) Integration of hole array with PDMS fluidic channel for initial prototype device.

To gauge the effectiveness of the technique a series of finite element based numerical simulations were conducted on the coupled low Reynolds number stokes flow, Eqs. (2), electrostatic, Eq. (3) and transient convection-diffusion-electrophoresis, Eq. (4), problem defined as below,

$$\eta\nabla^2 v - \nabla p = 0 \qquad (2a)$$

$$\nabla \cdot v = 0 \qquad (2b)$$

$$\nabla^2 \phi = 0 \qquad (3)$$

$$\frac{\partial c}{\partial t} = \nabla \cdot \left(D\nabla c + \mu_{ep} c \nabla \phi - cv \right) \qquad (4)$$

where v, t, p, ϕ, and c represent velocity, time, pressure electric potential and particle concentration respectively. η is the viscosity and D and μ_{ep} are the diffusivity (estimated using the Stokes-Einstein relation to be $5x10^{-11}$ m^2/s) and electrophoritic mobility of the quantum dots. The electrophoritic mobility can vary and be manipulated greatly depending on the suspension stabilization technique and conjugation, thus simulations were conducted for a series of different mobilities.

Figure 8 shows the computed potential field lines (for the purposes of these simulations the membrane layer has been omitted and microscale holes have been used) where a 1V potential difference has been applied at the bottom of a single active well and the edges of the fluidic system have been grounded. Insulation conditions were applied at all other boundaries. Simulation presented here were carried out in 2D. As is shown the applied potential field gradient is strongly concentrated within the trapping well and thus will serve to both attract the quantum dots, confine them once they are in place, and to reject them when the memory is to be erased (by reversing the polarity). The simulations revealed that in order to ensure that the majority of the potential drop occurs within the confinement well and not the channel, smaller relatively deep wells are preferable.

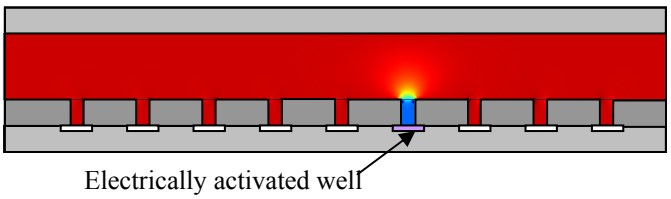

Figure 8: Computed applied potential field gradient with 1V applied at bottom of active storage well and channel grounded. The colored pad represents the activated well while all others are in the passive state (*i.e.* floating). The channel height is 10μm and the wells have a 2μm radius and 4μm depth. Computed potential field gradient within the well is $1x10^{-5}$ V/m.

The trapping effect is demonstrated in Figure 9 which shows timelaspe simulations of the system when a sample is convected over the trapping well array. As can be seen the quantum dots rapidly diffuse into both active and inactive wells. As the sample is convected away however the quantum dots rapidly diffuse out of the passive holes but remain indefinitely confined within the electrically active well. As can be seen the applied potential field also serves as a sample/signal concentrator increasing the local concentration of quantum dot's above that of the original sample. This concentration effect was found to be strongly influenced by the mobility of the quantum dots used (*i.e.* higher mobility serving to increase the concentration of the stored dots). In general however the simulations revealed that at the 1V potential difference limit imposed above, quantum dots with extremely low electrophoritic mobility (on the order of 10^{-9} m^2/Vs or lower) can be trapped via this technique.

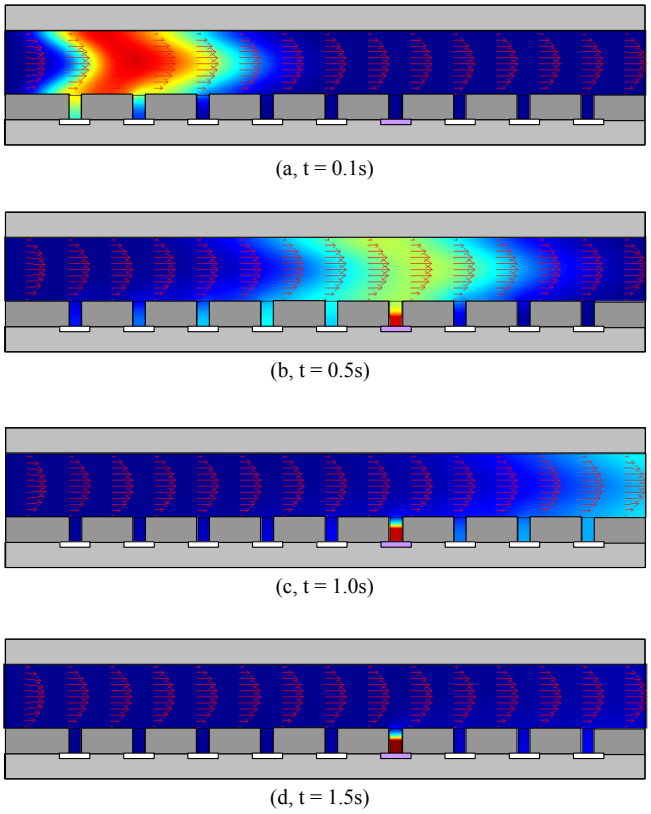

Figure 9: Timelapse images showing finite element simulations of electrostatic trapping scheme. Pressure driven flow is used to convect the sample over the trapping wells at an average velocity of 100μm/s. In these simulations a conservative estimate of the electrophoritic mobility of the quantum dots has been used ($\mu_{ep} = 5x10^{-10}$ m^2/Vs). Channel geometry is identical to that shown in Figure 8.

ACKNOWLEDGMENTS

The authors would like to thank Professor Axel Scherer for the use of the fiber spectrometer used to make the measurements shown in Figures 3 and 6. This work was carried out with funding from the DARPA Center for Optofluidics.

REFERENCES

[1] Maune, B. Lonkar M., Witzens J., Hochberg M., Baehr-Jones, T., Psaltis, D., Scherer, A., Qiu Y., 2004, "Liquid-crystal electric tuning of a photonic crystal laser" App. Phys. Lett., 85, pp. 360-362.

[2] Wolfe, D., Conroy, R., Garstecki, P., Mayers B., Fischbach, M., Paul, K., Prentiss, M., Whitesides, G., 2004 "Dynamic control of liquid-core liquid-cladding optical waveguides" PNAS-USA, 101, pp. 12434-12438

[3] Campbell, K., Groisman, A., Levy, U., Pang, L., Mookherjea, S., Psaltis, D., Fainman, Y., 2004, "A microfluidic 2x2 optical switch" App. Phys. Lett., 85, 6119-6121.

[4] Acharya, B., Krupenkin, T., Ramachandran, S., Wang, Z., Huang, C.C., Rogers, J., 2003, "Tunable optical fiber devices based on broadband long-period gratings and pumped microfluidics" App. Phys. Lett., 83, pp. 4912-4914.

[5] Unger, M., Chou, H., Thorsen, T., Scherer, A., Quake, S., 2000, "Monolithic microfabricated valves and pumps by multilayer soft lithography" Science, 288, pp. 113-116.

[6] Thorsen, T., Maerkl, S.J., Quake, S.R., 2002 "Microfluidic Large Scale Integration" Science, 298, pp. 580-584.

[7] Groisman, A., Enzelberger, M., Quake, S., 2003, "Microfluidic memory and control devices" Science, 300, p. 955-958.

[8] Mingyong, H., Xiaohu, G., Su, J. Nie, S., 2001, "Quantum-dot-tagged microbeads for multiplexed optical coding of biomolecules" Nature Biotech. 19, pp 631 – 635.

[9] Chang, S., Zhou, M, Grover, C., 2004, "Information coding and retrieving using fluorescent semiconductor nanocrystals for object identification" Optics Express, 12, pp. 143-148.

[10] Bruchez, M., Moronne, M., Gin, P., Weiss, S., Alivisatos, A. (1998) "Semiconductor nanocrystals as fluorescent biological labels" Science 281, pp. 2013-2016.

[11] Duffy, D., McDonald, J., Schueller, O., Whitesides, G., 1998, "Rapid prototyping of microfluidic systems in poly(dimethylsiloxane)" Anal. Chem. 70 pp. 4974-4984.

[12] Dai, J., Ito, T., Sun, L., Crooks, R., 2003, "Electrokinetic Trapping and Concentration Enrichment of DNA in a Microfluidic Channel" JACS, 125, pp. 13026-13027.